Virology 532 (2019) 108–117

Contents lists available at ScienceDirect

Virology

journal homepage: www.elsevier.com/locate/virology

A nuclear envelop-associated baculovirus protein promotes intranuclear lipid accumulation during infection

Toshihiro Nagamine*, Takehiko Inaba[1], Yasushi Sako

RIKEN, Wako-shi, Saitama, Japan

ARTICLE INFO

Keywords:
Baculovirus
BmNPV
AcMNPV
Bm5
Ac13
BION
Nuclear envelop
Intranuclear lipid
Bro-N
DUF3627

ABSTRACT

Although it has been well-accepted that baculoviruses produce a virus envelop within the nucleus, the redistribution of membrane lipids in infected cells has not been demonstrated. Here, we characterize a baculovirus protein (Bm5/Ac13: renamed BION; baculovirus protein associated with both the inner- and outer nuclear membranes) that localizes to both the inner- and outer nuclear membranes and show that the nuclear membrane (NE) protein promotes formation of a virus-induced intranuclear structure, the peristromal region (PR). Consistent with its role in virus envelopment, the PR was found to contain viral membrane proteins and lipids, suggesting PR formation proceeds through intranuclear lipid accumulation. About 50% of the cells infected with a *bion*-deficient virus exhibited no polyhedra production due to lack of the PR. Association of BION with the NE rather than the PR may contribute to the formation of the PR and polyhedra via NE-to-PR lipid transport.

1. Introduction

Baculoviruses are large insect-pathogenic DNA viruses. In many biological and chemical laboratories, baculovirus expression vectors have been employed for recombinant protein production. In addition to their utility as expression vectors, baculoviruses are intriguing because of their unique infection cycle - the production of two structurally and functionally distinct types of virions, occlusion derived virions (ODVs) and budded virions (BVs) (Blissard et al., 2000). Although the two virions have identical nucleocapsids assembled in the virus-induced intranuclear structure, the virogenic stroma (VS), they acquire their membranes in different ways. BVs obtain a membrane from the cellular plasma membrane through a budding process that mediates systemic (i.e., cell-to-cell) infection in an individual insect. In contrast, ODVs synthesize a membrane within another virus-induced intranuclear structure, the peristromal region (PR), and are then occluded in inclusion bodies (termed polyhedra for nucleopolyhedroviruses [NPV] and granules for granuloviruses [GV]) that are environmentally stable and mediate insect-to-insect infection in the field (Williams and Faulkner, 1997). While the BV plasma membrane budding process is similar to that of other enveloped viruses, intranuclear membrane formation of ODVs is quite unique and its underlying molecular mechanism remains elusive.

The baculovirus *Bombyx mori* nucleopolyhedrovirus (BmNPV) is a close relative of the prototype baculovirus, Autographa californica multiple nucleopolyhedrovirus (AcMNPV), and is thought to have recently arisen from AcMNPV (Nagamine and Sako, 2016). While the two viruses have very similar replication mechanisms as well as genomic DNA sequences, BmNPV replicates in *B. mori* cells whereas AcMNPV does not (Kondo and Maeda, 1991; Nagamine and Sako, 2016). Because the silkworm *B. mori* is a domesticated insect and the sericulture industry has optimized its rearing, BmNPV-based expression vectors are more advantageous for mass production of proteins in insects. BmNPV is therefore one of the most intensively studied baculoviruses.

In our previous systematic localization analyses of baculovirus proteins in BmNPV-infected *B. mori* (BmN) cells, we found a protein (Bm5/Ac13; renamed BION: baculovirus protein associated with both the inner- and outer nuclear membranes) that localizes specifically to the nuclear envelope (NE). Although it is a non-essential gene product, BION has been suggested to contribute to progeny virus production (Ono et al., 2012; Kokusho et al., 2016). In this study, we screened for BION NE localization signals by expressing serial GFP-BION deletion mutants and show that the protein has a multi-domain structure. In addition, we show that BION promotes PR formation by using a *bion*-deficient virus (Δ*bion*). Consistent with a role of the PR in virus envelopment, the region was found to contain lipids as well as viral

* Corresponding author. Cellular Informatics Laboratory, RIKEN, 2-1 Hirosawa, Wako, Saitama, 351-0198, Japan.
E-mail address: tnaga@riken.jp (T. Nagamine).
[1] Present address: Molecular Medicine and Cell Biology Laboratory, Division of Biological Science, Nara Institute of Science and Technology, 8916-5 Takayama-cho, Ikoma, Nara 630–0192, JAPAN.

https://doi.org/10.1016/j.virol.2019.04.006
Received 25 March 2019; Received in revised form 18 April 2019; Accepted 18 April 2019
Available online 25 April 2019
0042-6822/

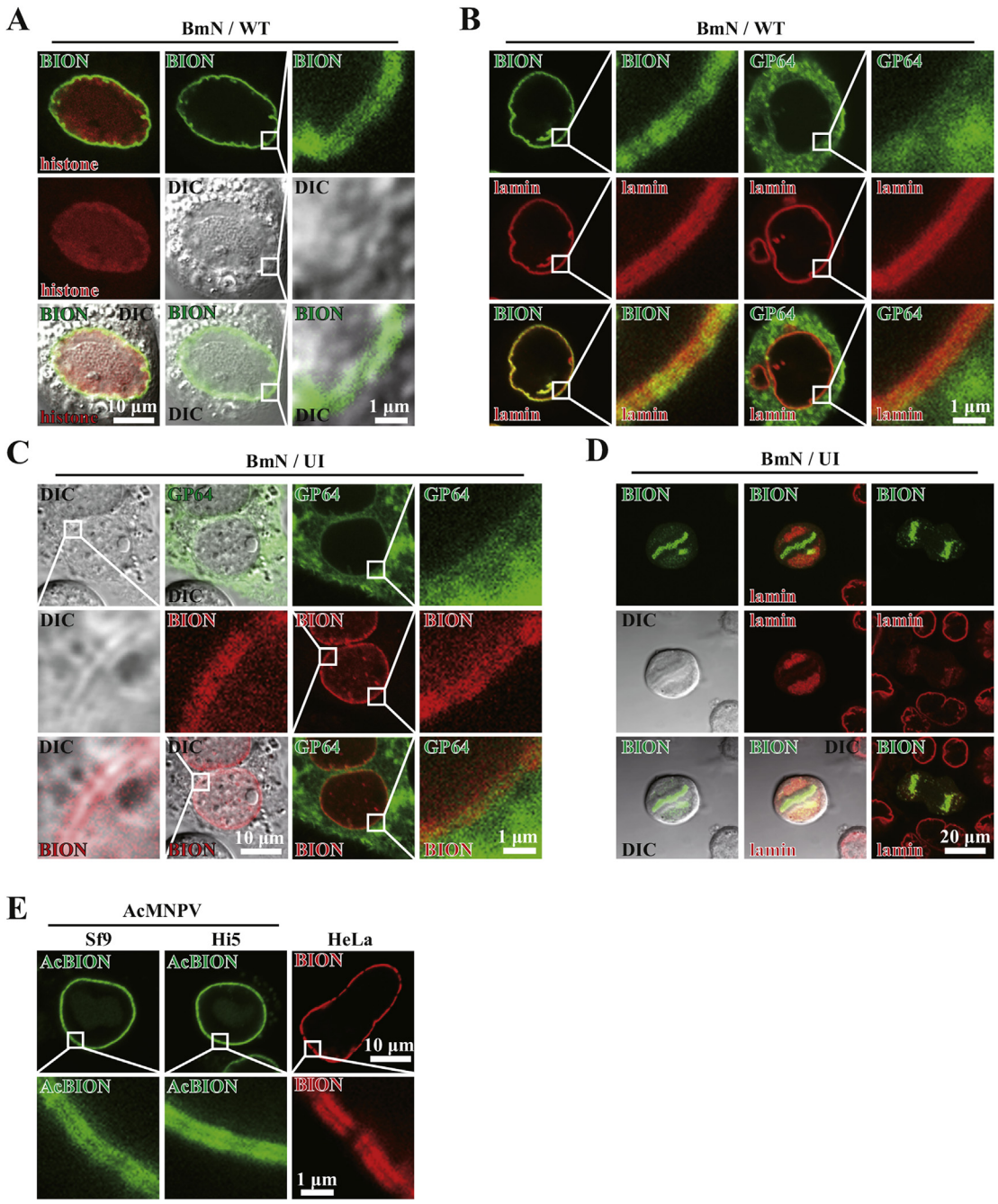

Fig. 1. Intracellular localization of BION. (A) Following transfection with plasmids expressing GFP-BION and DsRed-histone H4, BmN cells were infected with BmNPV. GFP-BION (BION) and histone H4-DsRed (histon) fluorescence images and differential interface contrast images (DIC) are shown. (B) Following transfection with a plasmid expressing GFP-BION or GP64-GFP, BmN cells were infected with BmNPV and stained with a Dm0 lamin antibody. GFP-BION (BION) and GP64-GFP (GP64) fluorescence images and anti-Dm0-antibody immunostaining images (lamin) are shown. (C) BmN cells were transfected with plasmids expressing Halo-BION and GP64-GFP and stained with Halo Tag TMR (tetramethylrhodamine) Ligand (Promega). Halo-BION (BION) and GP64-GFP (GP64) fluorescence images and differential interface contrast images (DIC) are shown. (D) BmN cells were transfected with a plasmid expressing GFP-BION and stained with a Dm0 lamin antibody. GFP-BION fluorescence images (BION), anti-Dm0-antibody immunostaining images (lamin) and differential interface contrast images (DIC) are shown. (E) Following transfection with a plasmid expressing GFP-AcBION, Sf9 cells (Sf9) and High Five cells (Hi5) were infected with AcMNPV. HeLa cells (HeLa) were transfected with a plasmid expressing Halo-BION and stained with Halo Tag TMR Ligand (Promega). GFP-AcBION (AcBION) and Halo-BION (BION) fluorescence images are shown. Infected cells and uninfected cells (UI) were analyzed by confocal microscopy at 24 h after infection and at 24 h after transfection, respectively.

membrane proteins. Since PR-deficient (but Δ*bion*-infected) cells exhibited neither intranuclear lipid accumulation nor polyhedra formation, BION likely plays a role in progeny virus production by facilitating PR formation. Because BION is a NE protein rather than a PR protein, it may contribute to PR and polyhedra formation via NE-to-PR lipid transport.

2. Results

2.1. BION is a NE-associated protein

In our systematic analysis of GFP-tagged baculovirus proteins, we found the BmNPV protein, BION (previously termed Bm5), localizes to both the inner and outer nuclear membranes, but neither the ER nor the

plasma membrane (Fig. 1A). Dual color imaging of GFP-tagged BION (GFP-BION) and an insect NE antigen stained with an anti-Dm0 (a *Drosophila* lamin protein) antibody confirmed NE localization of BION (Fig. 1B) as shown previously (Kokusho et al., 2016). To characterize this protein, we initially examined its temporal expression pattern by microscopy (Fig. S1). When BmN cells were infected with a wild-type virus (WT) following transfection with a plasmid expressing GFP-BION under the control of the authentic *bion* promoter, its NE localization was observed from 8 hpi and was maintained until at least 48 hpi (Fig. S1A). When this plasmid was introduced into uninfected cells, *bion* expression was regulated by IE1, the principal baculovirus transactivator (Fig. S1B). These results indicated that *bion* behaves as a delayed early and late gene as described previously (Zhou et al., 2010; Kokusho et al., 2016), though only the late promoter motif is found within 180 bp of the initiation codon (Gomi et al., 1999). When expressed under the control of the *Drosophila hsp70* promoter in uninfected cells, BION localized to the NE in interphase cells (Fig. 1C), revealing that BION can associate with the NE in the absence of other virus proteins. The baculovirus protein GP64, a type I integral membrane protein, localizes to the ER membrane and the plasma membrane in both uninfected- and infected cells (cf. Fig. 1B and C). Dual color imaging of GP64 and the Dm0 lamin antigen suggested localization to the ER and plasma membranes as well as NE localization (Fig. 1B). When co-expressed with GP64, BION localized to the boundary of the GP64-expressed nuclear periphery, indicating that the two proteins co-localize to the NE, possibly both the inner and outer nuclear membranes (Fig. 1C). In mitotic phase cells, BION associated with chromosomes (Fig. 1D), suggesting that it has a chromatin-binding domain. AcMNPV-BION (Ac13) also localized to the NE in both AcMNPV-infected Sf9 and High Five cells, suggesting that it functions similar to BmNPV-BION (Fig. 1E). BION similarly localized to the NE in a mammalian cell line (HeLa) (Fig. 1E), indicating that its NE localization mechanism is not insect-specific.

2.2. BION is a multi-domain protein

Since BION is associated with the NE and chromosomes, we screened for localization signals by expressing serial GFP-BION deletion mutants in uninfected and infected cells (Fig. 2). In uninfected cells, a BION mutant lacking the N-terminal 43 amino acids (Δ1-43), but which retained amino acids 44–331, was defective in NE localization and instead localized to the nucleoplasm. In contrast, a mutant possessing only the N-terminal 43 amino acids (Δ44-331) was cytoplasmic. Because the N-terminal 43-amino acid peptide (Δ44-331) exhibited an ER distribution pattern reminiscent of GP64 (see Fig. 1B and C) and is involved in NE localization, we concluded that this region comprises a membrane-binding domain. A mutant possessing only the C-terminal 44 amino acids (Δ1-287) was distributed throughout the cell similar to non-fused intact GFP, whereas another mutant possessing the C-terminal 98 amino acids (Δ1-233) exhibited a nucleoplasmic localization pattern. A mutant (Δ234-331) lacking the C-terminal 98 amino acids localized to the cytoplasm. These results and the association of BION with chromosomes in mitotic phase cells suggest that amino acids 234–288 contain a chromatin-binding domain. This domain, which spans residues 219–308, overlaps with a “domain of unknown function” in the Pfam database (i.e. DUF3627) (see Fig. 4A) and is found in various large DNA virus genomes (Finn et al., 2014), suggesting a possible function in chromatin-binding.

The NE localization profile was rescued by WT infection, but not *bion*-deficient BmNPV (Δ*bion*) infection, in cells expressing the Δ1-43 and Δ1-129 N-terminal truncation mutants, but not the Δ1-233 or Δ1-287 mutants. The NE localization profile was likewise rescued by WT (but not Δ*bion*) infection in cells expressing the Δ288-331 or Δ234-331 mutants. In contrast, no rescue was observed in cells expressing the Δ130-331 or Δ44-331 mutants. These results suggest that residues 130–233 contain a homophilic binding domain. It is unclear why the Δ288-331 mutant (44 amino acid C-terminal truncation) failed to localize to the NE; however, BION's NE-localization may depend on a specific conformational structure that is lost and/or obscured by the truncation.

2.3. BION has homophilic binding domains

The WT and Δ*bion* infection experiments in cells expressing the serial GFP-BION deletion mutants suggest that BION has a homophilic binding domain which mediates BION-BION interactions. To verify this, we performed co-expression experiments of the GFP-BION mutants with the intact untagged BION protein in uninfected cells. As expected from the results shown in Fig. 2, the Δ1-43, Δ1-129, Δ288-331 and Δ234-331 mutants localized to the NE in the presence of the intact BION protein, but the Δ1-233, Δ1-287 and Δ44-331 mutants did not (Fig. 3). These results confirmed that residues 130–233 contain a homophilic binding domain. Surprisingly, however, the Δ130-331 mutant localized to the NE in the presence of the intact BION protein even though WT infection failed to assist its NE localization. The region that spans amino acids 44–129 overlaps with a Bro-N (PF02498, BRO family, N-terminal domain) motif (aa 64–141) (see Fig. 4A). Bro-N motifs may, therefore, function as a homophilic binding domain that serves to interact between Bro-N-possessing proteins. Conceivably, NE localization of the Δ130-331 mutant may be disturbed by Bro-N-possessing proteins other than BION in WT-infected cells, where a number of Bro-N-possessing proteins are expressed.

2.4. A highly-conserved region in BION is required for NE localization

Within the putative homophilic binding domain (aa 130–233), we found a characteristic region (aa 185–215) highly conserved across baculoviruses (Fig. 4A). HHPred predicts that this region forms an α-helical structure with the N-terminal sequence (aa 185–199) forming a putative amphipathic helix (Fig. 4B) whereas the C-terminal portion (aa 200–215) resembles leucine zipper motifs (Fig. 4C). To examine whether this region contributes to the homophilic binding, we constructed plasmids expressing GFP-BIONs lacking the putative amphipathic helix region (AH; Δ185-199), the leucine zipper-like region (LZ; Δ200-215), and both regions (H&Z; Δ185-215). In uninfected cells, BION mutants lacking either the AH or LZ region localized to the nucleoplasm as well as the NE, suggesting that these regions contribute to NE localization to some degree (Fig. 4D and E). When both were deleted, the BION mutant no longer associated with the NE. These results suggest that the AH and LZ regions function synergistically in the NE localization of BION. In cells expressing these deletion mutants, their NE localization patterns were rescued by WT infection but not Δ*bion* infection (Fig. 4D), and they were also rescued by expression of intact BION in uninfected cells (Fig. 4E). These results indicate that the AH and LZ regions are non-essential for the homophilic binding of BION. However, it could be that BION mutants lacking AH and/or LZ are deficient in forming homophilic-associations between BION mutants rather than between an intact BION and the BION mutants.

2.5. BION promotes polyhedra production via PR formation

To further investigate BION function, we characterized Δ*bion* in BmN cells. Since a previous report suggests that BION supports virus replication mainly at the late stage of infection (Kokusho et al., 2016), we compared a late stage event, PR (peristromal region) formation, between WT- and Δ*bion*-infected cells. To account for differences in infectivity, we used a GFP-tagged ODV-E25 protein (GFP-E25) expressed under the control of the authentic late gene promoter (Kawasaki et al., 2004) as a marker of PR formation. This marker protein functions as an indicator for virus infection in addition to PR formation because it is expressed specifically in infected cells and localizes to the PR. At 48 h after WT infection, the PR was observed in most infected cells (87%); however, only 43% of Δ*bion*-infected cells

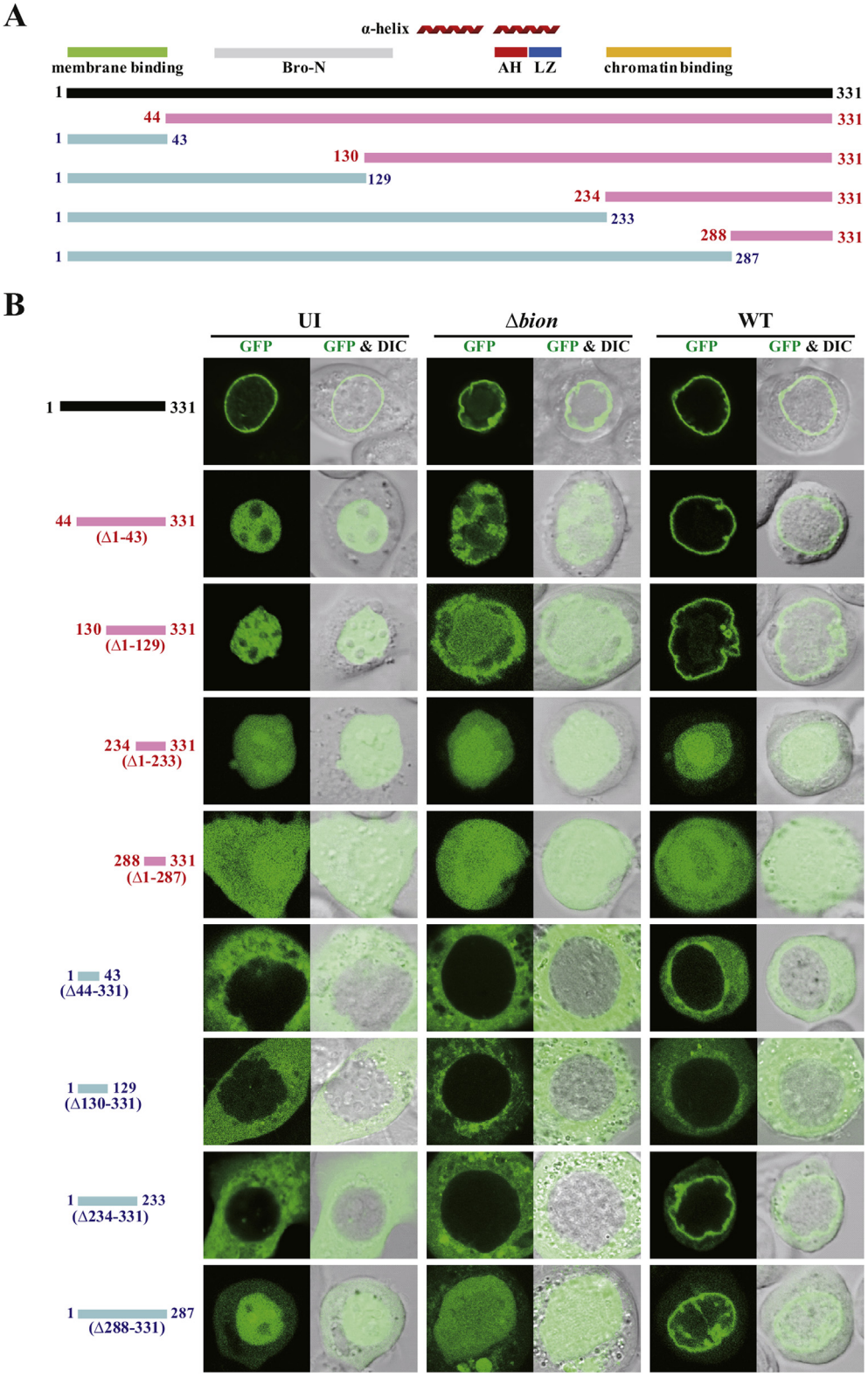

Fig. 2. Intracellular localization of serial deletion mutants of BION. (A) Schematic drawing of BION mutants. (B) BmN cells were transfected with a plasmid expressing the indicated GFP-BION mutant and analyzed by confocal microscopy without infection (UI) and at 24 h after infection with Δ*bion* (Δ*bion*) and wild-type BmNPV (WT).

exhibited PR formation, indicating that BION facilitates PR formation (Fig. 5A). When Halo-tagged BION was introduced into Δ*bion*-infected cells, the efficiency of PR formation was recovered (78%), confirming BION's role in PR formation (Fig. 5A). In the time course experiment of WT-infected cells, no PR was observed at 8 hpi, however, its formation was observed from 16 hpi (Fig. 5B). At 32 hpi, ~80% of WT-infected cells formed the PR. Similarly, no PR was observed at 8 hpi, but its formation was observed from 16 hpi in Δ*bion*-infected cells (Fig. 5B). Although > 40% of Δ*bion*-infected cells exhibited PR formation at 24 hpi, after that, little increase was observed in PR formation efficiency.

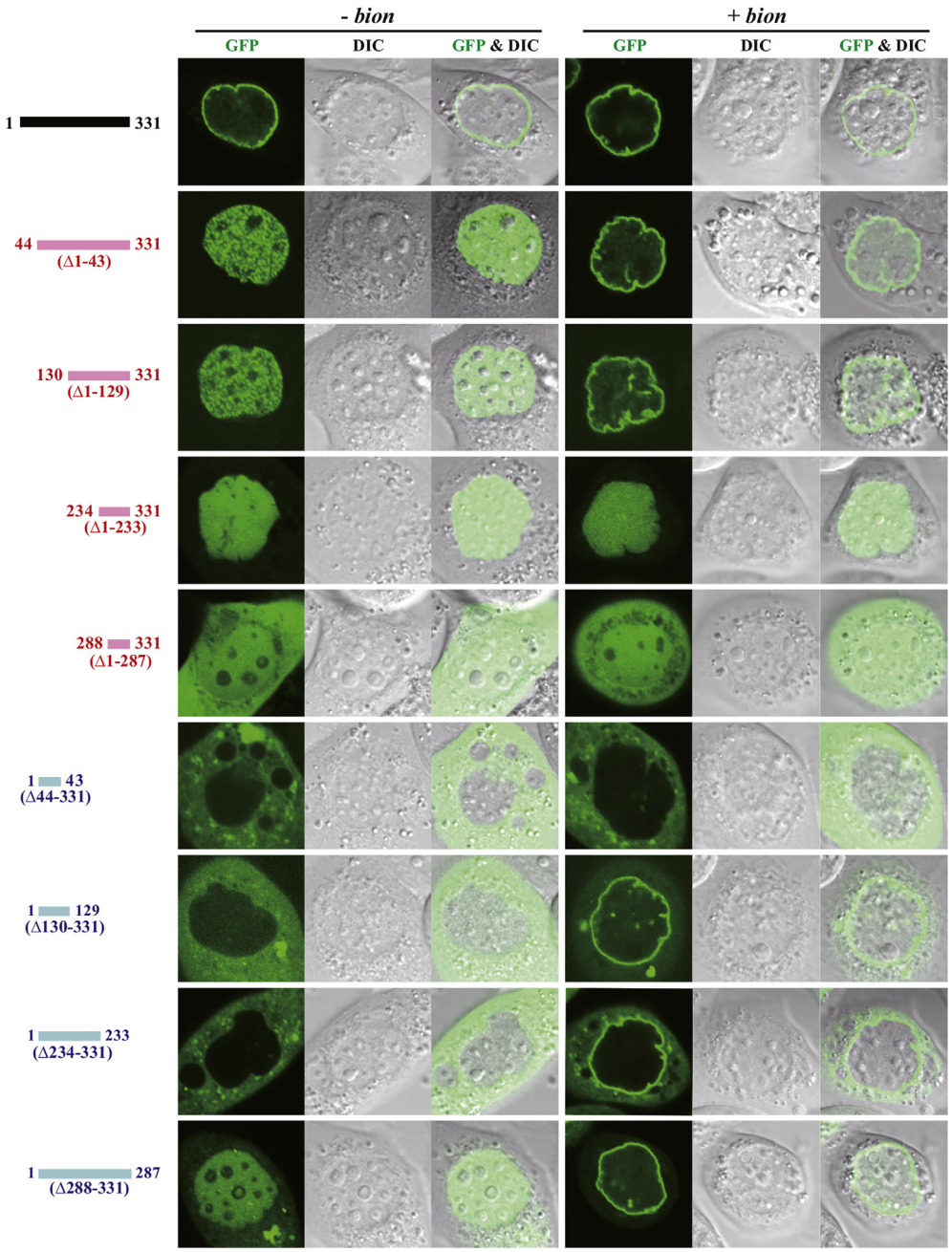

Fig. 3. Effects of intact BION expression on the localization of serial deletion mutants. BmN cells were transfected with plasmids expressing the indicated GFP-BION mutant and IE1 in the presence (+*bion*) or absence (- *bion*) of a plasmid expressing BION under the control of the authentic *bion* promoter and analyzed by confocal microscopy at 24 h post-transfection.

These results suggest that deletion of the *bion* gene restrains PR maturation but has little effect on the early stage of infection as describe previously (Kokusho et al., 2016).

Because it has been reported that BION is involved in polyhedra production (Kokusho et al., 2016), we also examined the relationship between PR formation and polyhedra formation in Δ*bion*-infected cells. To detect polyhedra clearly, cells were transfected with a plasmid expressing a DsRed-tagged polyhedrin protein in conjunction with the GFP-E25-expressing plasmid prior to virus infection. In WT-infected cells, polyhedra formed within (or close to) the PR, suggesting that initiation of polyhedra formation occurs within the PR (Fig. 5C). In Δ*bion*-infected cells, polyhedra were likewise associated with the PR, but were not observed in cells lacking the PR (Fig. 5C). In contrast, polyhedra-producing (but Δ*bion*-infected) cells always contained the PR (Fig. 5D). These results suggest that the PR is required for polyhedra formation and also that, in Δ*bion*-infected cells, the reduction of PR formation reflects lower polyhedra production.

2.6. The PR is an intranuclear lipid accumulation site

BION promotes polyhedra formation, probably via generation of the PR, which appears to be a cellular region associated with ODV membrane production (Kawasaki et al., 2004; Nagamine et al., 2008). Therefore, one possibility is that the PR is comprised of membrane lipids and that BION might function in PR lipid transport. To examine the lipid distribution of the PR, we treated BmN cells with a green fluorescent fatty acid (FA) (BODYPY FL C12) for 30 min immediately after WT infection and then observed at 4-h intervals. As shown in Fig. 6A, a

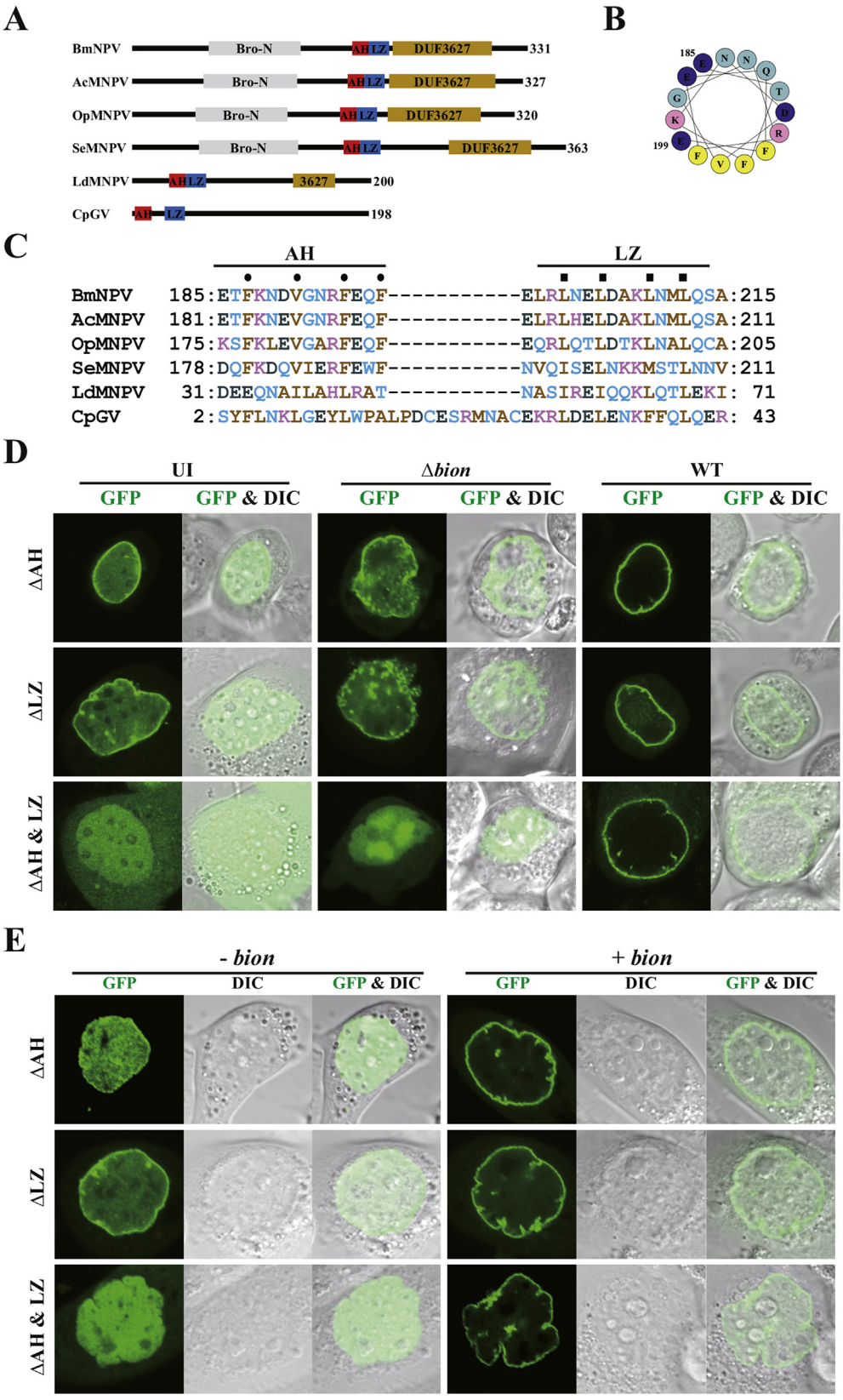

Fig. 4. Intracellular localization of BION mutants in which a highly-conserved region in baculoviruses was deleted. (A) Schematic drawing of baculovirus BIONs containing the putative amphipathic helix (AH), the putative leucine zipper motifs (LZ), the N-terminal domain of the BRO family (Bro-N), and DUF3627 (DUF3627 or 3627). (B) Helical wheel alignment of the putative amphipathic helix in BION. (C) Sequence alignment of the highly-conserved region in diverse baculovirus BIONs. (D) BmN cells were transfected with a plasmid expressing the indicated GFP-BION mutant and analyzed by confocal microscopy without infection (UI) and at 24 h after infection with Δ*bion* (Δ*bion*) and wild-type BmNPV (WT). (E) BmN cells were transfected with plasmids expressing the indicated GFP-BION mutant and IE1 in the presence (+*bion*) or absence (- *bion*) of a plasmid expressing BION under the control of the authentic *bion* promoter and analyzed by confocal microscopy at 24 h post-transfection. BmNPV; *Bombyx mori* NPV. AcMNPV; Autographa californica MNPV. OpMNPV; Orgyia pseudotsugata MNPV. SeMNPV; Spodoptera exigua MNPV. LdMNPV; *Lymantria dispar* MNPV. CpGV; Cydia pomonella GV.

lipid-accumulating region became observable in the nucleus at 12 hpi and gradually expanded until 24 hpi. This fluorescence pattern is similar to that reported in PR formation (Nagamine et al., 2008), and is consistent with lipid accumulation specific to the PR. To verify this, BmN cells expressing the PR marker protein GFP-E25 were stained with a red fluorescent FA (BODIPY 558/568 C12) 23.5–24 h after WT infection. In those cells, GFP-E25 co-localized with the intranuclear fluorescent lipids, confirming that the PR contains lipids (Fig. 6B). About 50% of the Δ*bion*-infected cells exhibited no PR formation (Fig. 5A). Those cells possessed little to no intranuclear lipids (Fig. 6B).

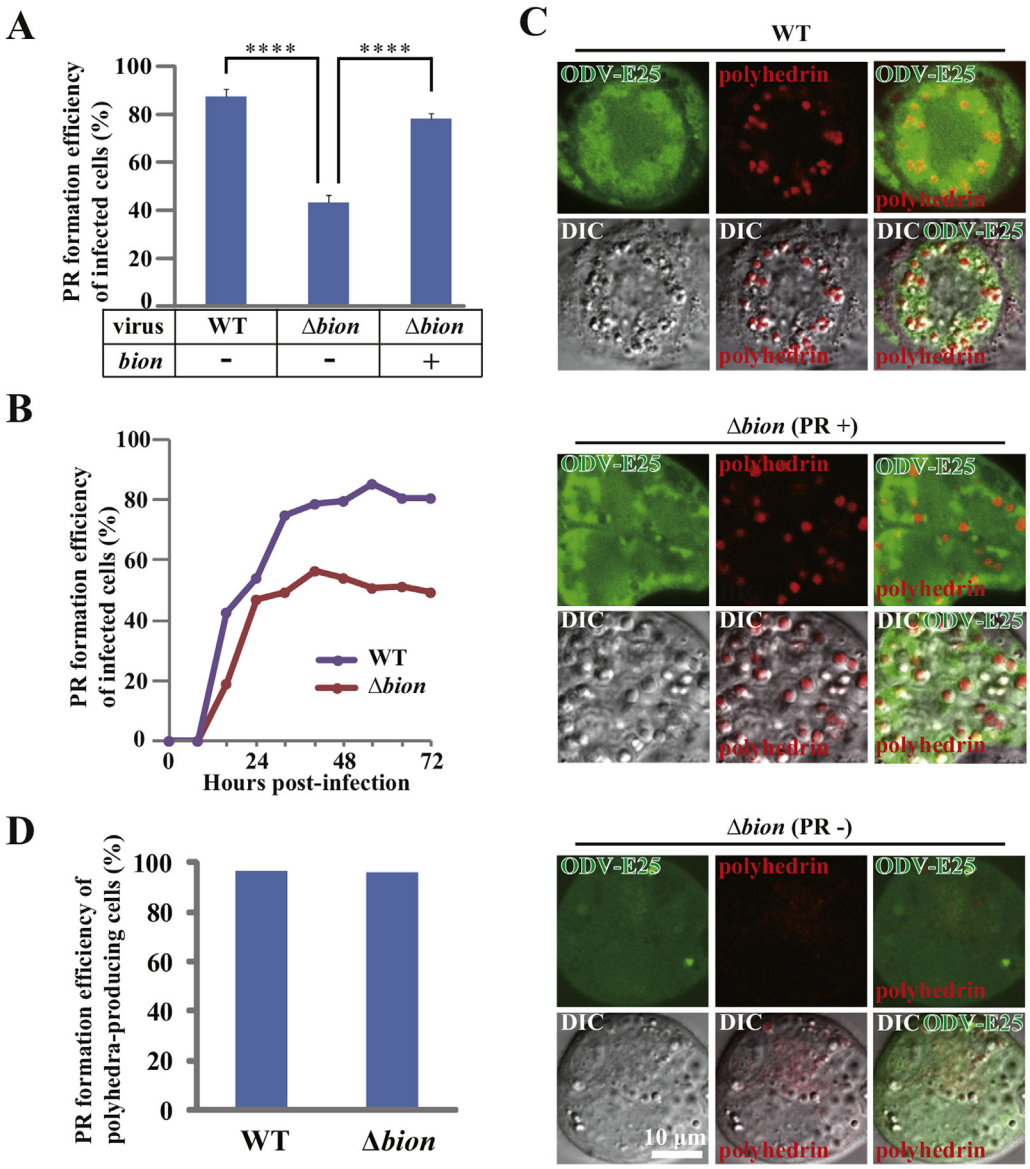

Fig. 5. A role of BION in PR formation and polyhedra production. (A) Bar graph showing the PR formation efficiency of infected cells. Following the indicated treatment, PR-possessing cells/infected cells were counted under fluorescent microscopy at 48 hpi. Two-sample *t*-test, $^{****}p < 0.0001$. (B) Time course plots of PR formation efficiency. BmN cells were transfected with a plasmid expressing GFP-E25 and PR-possessing cells/infected cells were counted under fluorescent microscopy at the designed time points. (C) BmN cells were transfected with plasmids expressing GFP-E25 and polyhedrin-DsRed and analyzed by confocal microscopy at 48 h after infection with wild-type BmNPV (WT) and Δ*bion* (Δ*bion*). PR-presence (PR +) and PR-absence (PR -) in Δ*bion*-infected cells are shown. (D) Bar graph showing PR formation efficiency of polyhedra-producing cells. BmN cells were treated as described in (C) and PR-possessing cells/polyhedra-producing cells were counted under fluorescent microscopy at 48 hpi.

This result indicates that PR formation is correlated with intranuclear lipid accumulation. Therefore, taken together with the data that BION is a NE protein rather than a PR protein, it is possible that BION contributes to PR formation through NE-to-PR lipid transport.

3. Discussion

It has been previously reported that BION is not a structural protein associated with BV or ODV (Zhou et al., 2010) and that it localizes to the NE in infected cells (Kokusho et al., 2016). While *bion* has been classified as a non-essential gene (Ono et al., 2012; Kokusho et al., 2016), it has been demonstrated that *bion* disruption results in lower titers of BV and a reduction in polyhedra (Kokusho et al., 2016). In this report, we characterized various BION deletion mutants to identify NE localization signal(s) and demonstrate that BION plays a role in PR and polyhedra formation by using a *bion*-deficient virus.

BION localized to both the inner nuclear membrane (INM) and the outer nuclear membrane (ONM) but did not localize to the ER or the plasma membrane. A number of ODV envelope proteins with an INM localization sorting motif (INM-SM) are thought to be integrated into the ER membrane prior to PR localization (Braunagel et al., 2004; Saksena et al., 2004). BION, however, does not appear to be integrated into the ER membrane co-translationally as the protein lacks both a predictable signal sequence and a transmembrane helix such as INM-SM. Instead, BION possesses an N-terminal membrane-binding domain. Retention of only this domain results in ER localization, whereas intact BION exhibits NE localization, which suggests that NE localization requires cooperative interactions across its multiple domains. By searching the Pfam database, several motifs were found in the BION protein sequence. Bro-N (PF02498, BRO family, N-terminal domain) motifs are detected in BRO family proteins as well as other baculovirus proteins such as Orf22 of Cydia pomonella GV (CpGV). Since co-expression of the intact BION protein facilitated NE localization of the Δ130-331 mutant, but not the Δ44-331 mutant, in uninfected cells, BION's Bro-N (aa 64–141) domain seems to function in its homophilic association. In WT-infected cells, however, the Bro-N homophilic association between the intact BION protein and the Δ44-331 mutant may be disturbed by Bro-N-possessing proteins other than BION. In the other putative homophilic binding domain (aa 130–233), three motifs (Allexi-40kDa [PF5549, aa 151–237; Allecivirus 40 kDa protein], CENP-F_leu_zip [PF10473, aa 152–214; Leucine-rich repeats of kinetochore protein Cenp-F/LEK1], and CLZ [PF16526, aa 151–200; C-terminal leucine zipper domain of cyclic nucleotide-gated channels]) overlapped. Structural similarities with these motifs suggest that the

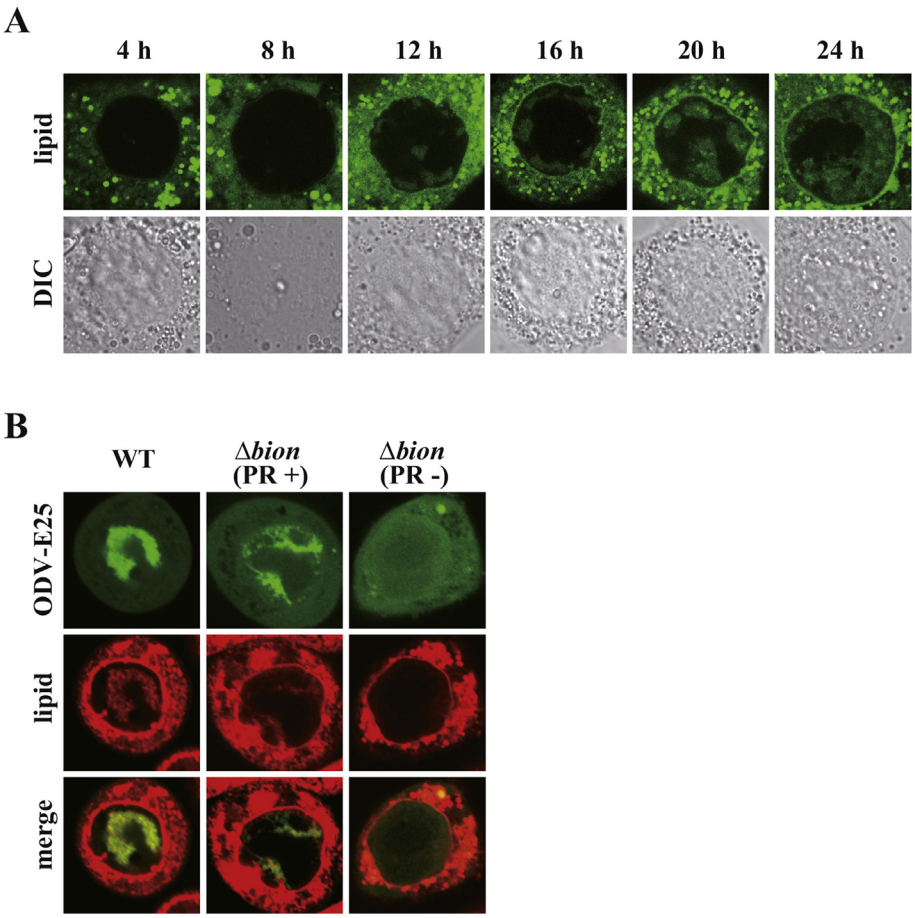

Fig. 6. Lipid accumulation in the PR. (A) BmN cells were stained with a green fluorescent fatty acid (BODYPY™-FL C12) for 30 min immediately after WT infection and then analyzed by confocal microscopy at the indicated time points post-infection. (B) Following transfection with a plasmid expressing GFP-E25, BmN cells were stained with a red fluorescent FA (BODIPY 558/568 C12) for 23.5–24 h post-infection with wild-type BmNPV (WT) and Δ*bion* (Δ*bion*) and analyzed by confocal microscopy. PR-presence (PR +) and PR-absence (PR -) in Δ*bion*-infected cells are shown.

putative homophilic binding domain in BION facilitates protein-protein interactions. On the other hand, it is likely that INM localization requires cooperativity between the DUF3627 (aa 219–308) domain, which appears to function in chromatin-binding, and the N-terminal membrane-binding domain. Once BION localizes to the INM, it may diffuse freely to the ONM through the nuclear pores. Because the perinuclear space (PNS) between the INM and the ONM is generally around 30–50 nm (Franke et al., 1981), light microscopy-based discrimination of the two membrane is often challenging. Nevertheless, the two membranes could be distinguished under our conditions. The INM, the PNS, and the ONM might possess quite different optical properties, which could be the reason for the discrimination between the two membranes.

Previously, we reported that the PR was a virus-induced nuclear structure to which viral envelope proteins localize (Nagamine et al., 2008). Because it has been demonstrated that disruption of *bion* has effects on progeny virus production rather than viral genome replication (Kokusho et al., 2016), we examined PR formation in Δ*bion*-infected cells. These cells exhibited reduced PR formation relative to WT-infected cells and PR-absent cells displayed neither intranuclear lipid accumulation nor polyhedra formation. However, polyhedra-producing (but Δ*bion*-infected) cells always contained the PR, revealing that the PR is required for polyhedra formation. These results suggest that the reduced PR formation in Δ*bion*-infected cells accounts for the lower numbers of polyhedra (and presumably ODV due to the lack of PR lipids) in comparison to WT-infected cells (Kokusho et al., 2016). Kokusho et al. (2016) also reported that both BV and polyhedra production were decreased in Δ*bion*-infected cells. While the relationship between BV production and PR formation is still unknown, one possibility for the lower BV titers in Δ*bion*-infected cells is that BION could play a role in BV production via a mechanism other than PR formation such as promoting nuclear egress of BVs.

BION promotes PR formation even though it localizes to the NE rather than the PR. A previous report demonstrated that a mutant BmNPV lacking only the DUF3627 region (BION's chromatin binding domain) of BION reduced polyhedra formation (Kokusho et al., 2016), possibly due to cytosolic localization of the mutant. This observation suggests that NE localization of BION is essential for efficient polyhedra production. Since BION seems to function specifically in the NE and PR formation is correlated with intranuclear lipid accumulation, BION may contribute to lipid transport from the NE to the PR. In addition to the PR, baculoviruses produce another nuclear structure, the virogenic stroma (VS), in which viral DNA replication and capsid assembly occur (Williams and Faulkner, 1997). In infected cell nuclei, the VS, the PR, and cellular chromatin never overlap (Nagamine et al., 2008). In the course of virus infection, the VS and the PR expand sequentially, resulting in marginalization of cellular chromatin within the nucleus (Nagamine et al., 2008). VS expansion depends upon viral DNA synthesis (Okano et al., 1999; Nagamine et al., 2008). Because the PR contains both viral envelope proteins and lipids, its expansion may depend on lipid accumulation rather than DNA accumulation. If lipid accumulation is required for PR expansion, BION may assist PR formation through lipid-dependent PR expansion. Furthermore, because BION is associated with the NE in the absence of other viral proteins and in NE-to-PR transport, it might function as a NE scaffolding structure for NE-to-PR lipid transport in infected cells. The PR formation observed in some Δ*bion*-infected cells could suggest more inefficient assembly of the machinery necessary for NE-to-PR transport in the absence of BION. Because BmN cells are an uncloned cell line, this differential BION dependency might be cell-type specific. Kokusho et al. (2016), however, reported the reduction of polyhedra formation efficiency in Δ*bion*-infected insects. Hence, even If the BION's function

might be cell-type specific, insects would have BION-dependent cells in which the protein promotes PR-reliant polyhedra production.

In many cells, lipids accumulate in the cytoplasm as lipid droplets, which are spherical and surrounded by a lipid monolayer. On the other hand, the PR is likely to have a structure different from lipid droplets. One possibility is that it contains numerous membrane vesicles as a lipid reservoir, which may account for why the PR is non-spherical. If so, BION may facilitate NE-to-PR vesicle transport via a vesicle-budding process in the NE, which would be quite unique. Thus, our data provide a novel insight into vesicle trafficking in baculovirus-infected cells and offer a clue for studying the complex processes of ODV membrane production in the nuclei.

4. Materials and methods

4.1. Cells and viruses

BmN cells were maintained in TC100 medium (Funakoshi) supplemented with 10% FBS (Kawasaki et al., 2004), and Sf9 and High Five cells (Invitrogen) were maintained in SF900-II (Invitrogen) (Nagamine et al., 2005). HeLa cells were maintained in D-MEM (Wako) supplemented with 10% FBS. The BmNPV wild-type isolate T3 (Kondo and Maeda, 1991) and the AcMNPV wild-type isolate E2 (Smith and Summers, 1978) were propagated in BmN cells and Sf9 cells respectively. The *bion* (Bm5)-deficient BmNPV (Δ*bion*/Bm5D) was generated as described previously (Kokusho et al., 2016). In the mutant virus, *bion* was disrupted by insertion of a *hsp70-lacZ* cassette (3.7 kbp) (Kamita et al., 1993) into amino acids 126–181 of its open reading frame (Kokusho et al., 2016).

4.2. Plasmid construction

The plasmids expressing histone H4-DsRed (pIB-BmH4-DsR) and GFP-E25 (pPES-oe25-GFP) were constructed as described previously (Kawasaki et al., 2004; Nagamine et al., 2008). The plasmid expressing a GFP-tagged BION protein (GFP-BION) under the control of the authentic *bion* promoter (*pbion*:GFP-BION) was derived from a BmNPV genomic fragment (EEbs14: map unit 0.02–0.05). The 12 bp 5′-flanking region (immediately in front of the initiation codon) of *bion* in the genomic fragment was replaced with dual XhoI-SpeI sites by site-directed mutagenesis and the *GFP* open reading frame from pEGFP-1 (Clontech) was inserted into the restriction site. To construct plasmids expressing GFP-BION and GFP-AcBION under the control of the *Drosophila hsp70* promoter (*phsp70*:GFP-BION and *phsp70*:GFP-AcBION respectively), BmNPV genomic fragment EEbs14 (map unit 0.02–0.05) and whole AcNPV-E2 genomic DNA were used as templates. PCR was performed with KOD DNA polymerase (Toyobo) and the primers Xho-ORF5-F and Bgl-ORF5-R (PCR primers used in this study are listed in Table 1). The resultant PCR products were inserted into the SalI-BamHI sites of pHE-C, a pEGFP-C1 (Clontech)-derived plasmid (Nagamine et al., 2011). Plasmids expressing a Halo-tagged BION protein (Halo-BION) under the control of the *Drosophila hsp70* promoter and the mammalian CMV promoter were constructed by insertion of the PCR product containing the *bion* open reading frame into the SalI-BamHI sites of pHE-C and pHalo7-C1 respectively. pHalo7-C1 was produced by replacement of the *GFP* open reading frame in pEGFP-C1 with the HaloTag open reading frame from the pFN19K HaloTag T7 SP6 Flexi Vector (Promega). The plasmid expressing a GFP-tagged GP64 protein (GP64-GFP) under the control of the authentic *gp64* promoter (*pgp64*:GP64-GFP) was derived from a BmNPV genomic fragment (map unit 77.7–83.3). The 13 bp sequence containing the termination codon (underlined) of the *gp64* gene (TAAATGTAATAAT) in the genomic fragment was replaced with HindIII-NheI sites (AAGCTTTGCTAGC) by site-directed mutagenesis and the *GFP* open reading frame from pEGFP-1(Clontech) was inserted into the restriction sites. Plasmids expressing serial deletion mutants of BION were constructed in the same manner as the plasmid expressing *phsp70*:GFP-BION except with unique PCR primers (Table 1). To create the plasmids expressing BION mutants lacking AH (aa 185–199), LZ (aa 200–215) and both AH and LZ (aa 185–215), a plasmid expressing *phsp70*:GFP-BION was used as the template and inverse PCR was performed with the primer sets ORF5-552-532/ORF5-598-618, ORF5-597-576/ORF5-646-667, and ORF5-552-532/ORF5-646-667 respectively. The resultant PCR products were ligated and employed for transformation to generate the desired plasmids. The plasmid expressing a DsRed-tagged polyhedrin protein (Polh-DsR) under the control of the authentic *polyhedrin* promoter was derived from a BmNPV genomic fragment (map unit 96.8–5.2). The 12 bp sequence containing the termination codon (underlined) of the *polyhedrin* gene (TAAAACACTATA) in the genomic fragment was replaced with XhoI-NheI sites (CTCGAGGCTAGC) by site-directed mutagenesis and the *DsRed* open reading frame from pDsRed2-1 (Clontech) was inserted into the restriction sites. All of the plasmids were confirmed by restriction enzyme analysis and DNA sequencing.

Table 1
PCR primers.

Primer	Sequences (5′ to 3′)
Xho-ORF5-F	GGCTCGAGATGCTATCCTGGTTATGGAATTG
Bgl-ORF5-R	GGAGATCTTTACAATACTTCTTGTATAACCTC
Xho-ORF5-F44	GGCTCGAGATGCAATGGTCGCACATCGTTAAATG
Xho-ORF5-F130	GGCTCGAGATGGGGTTGTTGAAAATTTTGATGC
Xho-ORF5-F234	GGCTCGAGATGCCGCGCGACATTACCAAAC
Xho-ORF5-F288	GGCTCGAGATGCCCTTGTTGGCAATTCAATG
Bgl-ORF5-R43	GGAGATCTTTATTGGACGTTTATGTGGTACTT
Bgl-ORF5-R129	GGAGATCTTTACTGCTTGGTCGCGAACAATG
Bgl-ORF5-R233	GGAGATCTTTAAAACGTCACCGTGCCATTTTTG
Bgl-ORF5-R287	GGAGATCTTTAATTTGGGTGCACACCGTCATAG
ORF5-552-532	GTGGGTGACCATAAATTTTTC
ORF5-598-618	TTGCGTTTGAACGAACTCGAC
ORF5-597-576	TTCAAACTGCTCAAACCTGTTG
ORF5-646-667	GAAAAATTGAAAACCGCCATCG

4.3. Transfection, infection, immunostaining, lipid labeling, and microscopy

Plasmid transfection and virus infection of insect cells were performed as described previously (Kawasaki et al., 2004). In all infection experiments, time zero was defined as the time point at which fresh medium was added following the 1-h virus adsorption period. HeLa cells were transfected with the FuGENE transfection reagent according to the manufacturer's instructions (Promega). HaloTag staining was conducted with the HaloTag TMR Ligand according to the manufacturer's instructions (Promega). Immunostaining was performed as described previously (Nagamine et al., 2005) using a 1:25 dilution of an anti-Dm0 antibody (ADL67.10: DSHB) as the primary antibody and a 1:200 dilution of a TMR-conjugated goat-anti-mouse IgG antibody (Cappel) as the secondary antibody. For lipid labeling with green fluorescent fatty acids, BmN cells were stained immediately after the 1-h virus adsorption period with 5 μM of BODYPY FL C12 (Molecular Probes) for 30 min and the labeling medium was replaced with fresh medium after staining. For red fluorescent fatty acids, BmN cells were transfected with a plasmid expressing GFP-E25 then subsequently infected with WT or Δ*bion* and stained with 5 μM BODIPY 558/568 C12 (Molecular Probes) for 23.5–24 hpi. Confocal images were acquired with a Leica TCS SP2 AOBS (63×, 1.4 NA, oil) using a 488-nm laser line for GFP and BODYPY FL and a 543-nm laser line for DsRed, tetramethylrhodamine (TMR) and BODIPY 558/568.

Fig. S1. Temporal expression pattern of BION. (A) Following transfection with plasmids expressing GFP-BION and DsRed-histone H4, BmN cells were infected with BmNPV and analyzed by confocal microscopy at the indicated time points post-infection. (B) IE1 dependency of the *bion* promoter. BmN cells were transfected with a plasmid expressing GFP-BION under the control of the authentic *bion*

promoter in the presence (+IE1) or absence (-IE1) of a plasmid expressing IE1 and analyzed by confocal microscopy at 48 h post-transfection.

Acknowledgments

We thank J. Joe Hull for critical reading of the manuscript. This research was supported in part by JSPS KAKENHI Grant Number 17K08162.

Appendix A. Supplementary data

Supplementary data to this article can be found online at https://doi.org/10.1016/j.virol.2019.04.006.

References

Blissard, G.W., Black, B., Crook, N.E., Keddie, B.A., Possee, R.D., Rohrmann, G.F., Theilmann, D., Volkman, L., 2000. In: Regenmortel, M.H.V.V. (Ed.), Family Baculoviridae in Virus Taxonomy: Seventh Report of the International Committee on Taxonomy of Viruses. Academic Press, San Diego, Calif, pp. 195–202.

Braunagel, S.C., Williamson, S.T., Saksena, S., Zhong, Z., Russell, W.K., Russell, D.H., Summers, M.D., 2004. Trafficking of ODV-E66 is mediated via a sorting motif and other viral proteins: facilitated trafficking to the inner nuclear membrane. Proc. Natl. Acad. Sci. U.S.A. 101, 8372–8377.

Finn, R.D., Bateman, A., Clements, J., Coggill, P., Eberhardt, R.Y., Eddy, S.R., Heger, A., Hetherington, K., Holm, L., Mistry, J., Sonnhammer, E.L., Tate, J., Punta, M., 2014. Pfam: the protein families database. Nucleic Acids Res. 42, D222–D230.

Franke, W.W., Scheer, U., Krohne, G., Jarasch, E.D., 1981. The nuclear envelope and the architecture of the nuclear periphery. J. Cell Biol. 91, 39s–50s.

Gomi, S., Majima, K., Maeda, S., 1999. Sequence analysis of the genome of Bombyx mori nucleopolyhedrovirus. J. Gen. Virol. 80, 1323–1337.

Kamita, S.G., Majima, K., Maeda, S., 1993. Identification and characterization of the p35 gene of *Bombyx mori* nuclear polyhedrosis virus that prevents virus-induced apoptosis. J. Virol. 67, 455–463.

Kawasaki, Y., Matsumoto, S., Nagamine, T., 2004. Analysis of baculovirus IE1 in living cells: dynamics and spatial relationships to viral structural proteins. J. Gen. Virol. 85, 3575–3583.

Kokusho, R., Koh, Y., Fujimoto, M., Shimada, T., Katsuma, S., 2016. *Bombyx mori* nucleopolyhedrovirus BM5 protein regulates progeny virus production and viral gene expression. Virology 498, 240–249.

Kondo, A., Maeda, S., 1991. Host range expansion by recombination of the baculoviruses *Bombyx mori* nuclear polyhedrosis virus and *Autographa californica* nuclear polyhedrosis virus. J. Virol. 65, 3625–3632.

Nagamine, T., Abe, A., Suzuki, T., Dohmae, N., Matsumoto, S., 2011. Co-expression of four baculovirus proteins, IE1, LEF3, P143, and PP31, elicits a cellular chromatin-containing reticulate structure in the nuclei of uninfected cells. Virology 417, 188–195.

Nagamine, T., Kawasaki, Y., Abe, A., Matsumoto, S., 2008. Nuclear marginalization of host cell chromatin associated with expansion of two discrete virus-induced subnuclear compartments during baculovirus infection. J. Virol. 82, 6409–6418.

Nagamine, T., Kawasaki, Y., Iizuka, T., Matsumoto, S., 2005. Focal distribution of baculovirus IE1 triggered by its binding to the *hr* DNA elements. J. Virol. 79, 39–46.

Nagamine, T., Sako, Y., 2016. A role for the anti-viral host defense mechanism in the phylogenetic divergence in baculovirus evolution. PLoS One 11, e01563942.

Okano, K., Mikhailov, V.S., Maeda, S., 1999. Colocalization of baculovirus IE-1 and two DNA-binding proteins, DBP and LEF-3, to viral replication factories. J. Virol. 73, 110–119.

Ono, C., Kamagata, T., Taka, T., Sahara, K., Asano, S., Bando, H., 2012. Phenotypic grouping of 141 BmNPVs lacking viral gene sequences. Virus Res. 165, 197–206.

Saksena, S., Shao, Y., Braunagel, S.C., Summers, M.D., Johnson, A.E., 2004. Cotranslational integration and initial sorting at the endoplasmic reticulum translocon of proteins destined for the inner nuclear membrane. Proc. Natl. Acad. Sci. U.S.A. 101, 12537–12542.

Smith, G.E., Summers, M.D., 1978. Analysis of baculovirus genomes with restriction endonucleases. Virology 89, 517–527.

Williams, G.V., Faulkner, P., 1997. Cytological changes and viral morphogenesis during baculovirus infection. In: Miller, L.K. (Ed.), The Baculoviruses. Plenum Press, New York, pp. 61–107.

Zhou, Y., Chen, K., Yao, Q., Shen, H., Liang, G., Li, X., Wang, N., Li, Y., 2010. Characterization of a late expression gene of *Bombyx mori* nucleopolyhedrovirus. Z. Naturforsch. C Biosci. 65, 508–518.